



## ANALYSIS OF 3D NONLINEAR RC CONCRETE STRUCTURES CONSIDERING GROUND MOTION DURATION

M. Fairhurst<sup>(1)</sup>, A. Bebamzadeh<sup>(2)</sup>, C. E. Ventura<sup>(3)</sup>

<sup>(1)</sup> Ph.D. Candidate and Research Assistant, University of British Columbia, fairhurstmike@gmail.com

<sup>(2)</sup> Research Associate and Lecturer, University of British Columbia, armin@civil.ubc.ca

<sup>(3)</sup> Professor, University of British Columbia, ventura@civil.ubc.ca

### **Abstract**

Recent subduction zone megathrust earthquakes in Tohoku, Japan (Mw 9.1, 2011), El Maule, Chile (Mw 8.8, 2010), and Sumatra, Indonesia (Mw 9.1, 2004) have served as reminders that large magnitude, long duration earthquakes are possible in subduction tectonic zones around the world. Several recent studies have shown that different structural systems are more susceptible to damage and collapse when subjected to longer duration motions, even when compared to shorter motions of equal intensity (typically characterized through spectral values).

In this study, a novel method is used to produce suites long and short duration motions with equivalent spectral means and standard deviations. This method uses spectral matching and variable target spectra (VTS) to match the mean and standard deviation of a ground motion suite to a specified target. This ensures that the ground motion suites are spectrally equivalent and can be reliably used to assess the isolated effect of ground motion duration.

These suites are then used to run nonlinear dynamic analyses (NDA) on a full 3-dimensional 18 story RC coupled shearwall building model. The model uses fiber elements and rotational hinges to capture the nonlinear behavior of the structure, including cyclic and in-cycle degradation. Modeling of this degradation as well as second order (P-Delta) effects is essential to capture the full effect of ground motion duration. NDA results demonstrate the vulnerability of this type of structure when subjected to the different types of potential ground motions and are useful for seismic risk assessment.

*Keywords: RC shearwall buildings, nonlinear dynamic analysis, subduction megathrust earthquakes, ground motion duration.*



## 1. Introduction

The seismicity in Southwestern British Columbia (BC), Canada, is dominated by the subduction of the oceanic Juan de Fuca plate beneath the continental North America plate occurring about 100 km west of Southern Vancouver Island – also called the Cascadia Subduction Zone. Both subduction and crustal events are possible - and have been recorded, or inferred - in this region. Crustal events occur in shallow faults in the Earth's crust and are typically less than magnitude (Mw) 8 with a short shaking duration (35 s significant duration or less). Subduction interface events can be much larger in magnitude (up to magnitude 9 [1]) and produce much longer shaking durations (on the order of 35 – 100 s significant duration).

Recent studies have shown that different structural systems are more susceptible to damage and collapse when subjected to longer duration motions, even when compared to shorter motions of equal intensity (typically characterized through spectral values) [2-5]. These studies, along with recent earthquakes located in subduction zones; such as Tohoku, Japan (Mw 9.1, 2011), El Maule, Chile (Mw 8.8, 2010) and Sumatra, Indonesia (Mw 9.1, 2004); have raised concerns over the design of structures located in subduction zones, as ground motion duration is typically not accounted for in modern North American building codes.

In this study, a novel algorithm is used to produce code-level suites of short (crustal) and long duration (subduction interface) ground motions. These suites are then used to run nonlinear dynamic analyses (NDA) on a 3-dimensional (3D), 18 story coupled reinforced concrete (RC) shearwall building model. The model uses fiber elements and rotational hinges to capture the nonlinear behavior of the structure, including cyclic and in-cycle degradation. The results are then used to assess and compare the performance of this type of structure under the two types of motions.

## 2. Numerical Model

### 2.1 Archetype Building

The building modeled for this study was an 18 story reinforced concrete shearwall building, typical of an existing residential building in Vancouver, BC. The lateral load resisting system includes three interior reinforced concrete shearwalls which comprise the elevator and stair core of the building. The gravity resisting system of the building includes circular perimeter and interior columns and 8" slabs at each story. The floor area is about 5200 ft<sup>2</sup> per story and the weight was calculated as 0.21 kips/ft<sup>2</sup> (approximately 10 kN/m<sup>2</sup>). The floor plan is illustrated in Figure 1a.

The building was designed using the equivalent lateral force procedure (ELFP) for a base shear calculated in accordance with the 2010 National Building Code of Canada (NBCC) for Vancouver, BC based on conventionally constructed coupled walls [6]. The seismic force reduction factor ( $R_d R_o$ ) of this system is 1.95. Reinforcement in the shearwalls for building is illustrated in Figure 1b. The walls are connected by 2' deep header beams which are reinforced by transverse 15M stirrups spaced at 4".

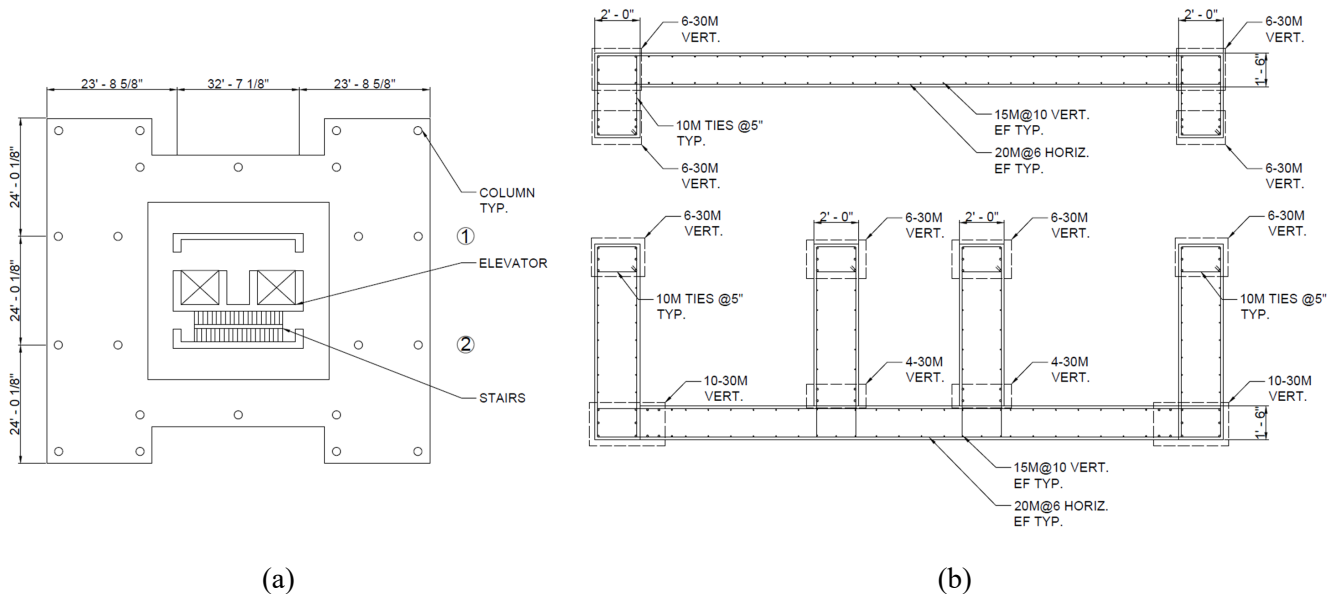


Fig. 1 - Archetype building a) floor plan, and b) shearwall reinforcement

## 2.2 Numerical Model

The OpenSees framework [7] was used to develop a 3D numerical model for the archetype building, similar to the 2-dimensional (2D) model developed by Fairhurst et al. [4]. The interior shearwalls were modeled using fiber elements with a displacement-based formulation and elastic shear hinges to capture elastic shear deformations. The elastic shear hinges had a stiffness reduced to 0.1 times their elastic stiffness to account for cracking [8].

The header beams were modeled using elastic beam elements with nonlinear shear hinges to account for the shear yielding and nonlinearity in the elements. The elastic beam elements were modeled considering a cracked section modulus ( $I_{\text{cracked}} = 0.35I_{\text{gross}}$ ) [9]. Rigid beam elements were used to connect the header beams to the walls in order to account for the physical width of the walls.

The nonlinear shear hinge properties were calibrated to a reverse-cyclic test on a similar beam performed by Galano and Vignoli [10] using the Pinching4 material model [11]. This model is able to capture capture pinching, in-cycle degradation, and cyclic stiffness and strength degradation. A comparison of the test results to the calibrated Pinching4 material model is presented in Figure 2a.

Concrete was modeled using the Concrete02 material model in OpenSees [12]. Confinement was accounted for using the Mander et al. relationship [13]. Both crushing and spalling are captured in this material model. Reinforcing steel was modeled using the ReinforcingSteel material model which can account for cyclic fatigue [14]. Buckling and fracture of the reinforcement was captured through the use of the MinMax material. To do this, the MinMax material was set to return zero strength and stiffness when the strain in the steel material reached the concrete crushing strain (assuming steel buckling will occur immediately after the surrounding concrete crushes) or the steel fracture strain [8]. Bar slip was modeled using a zero-length fiber section at the base of each wall using the Bond SP01 material model for the steel bars following Zhao and Sritharan [15].

The gravity system was also explicitly modelled. Columns were modelled as elastic elements with cracked stiffness values and nonlinear rotational hinges at each end. The backbone curve for these elements was based on ASCE 41-13 [16] recommendations and a bilinear material (Steel01) was used to model hysteretic behavior. Beam elements were used to model the outrigger, through slabs, between the column and wall elements. These beam elements comprised four components: 1) a nonlinear spring at the wall end; 2) an elastic beam representing the slab-beam width at the wall end; 3) an elastic beam representing the slab-beam



width at the column end; and, 4) a nonlinear rotational spring at the column end. The width of the elastic elements was based on the width of the wall/column they attached to, and the springs were modelled with the Steel01 material model and backbone curves from ASCE 41-13.

Damping was applied as 2.5% Rayleigh damping in the first and seventh modes (first two lateral modes in the coupled direction). The first three periods of the model were 1.06 s (coupled direction first lateral mode), 0.96 s (non-coupled direction first lateral mode), and 0.51 s (first torsional mode). An illustration of a typical story of the OpenSees model is presented in Figure 2b.

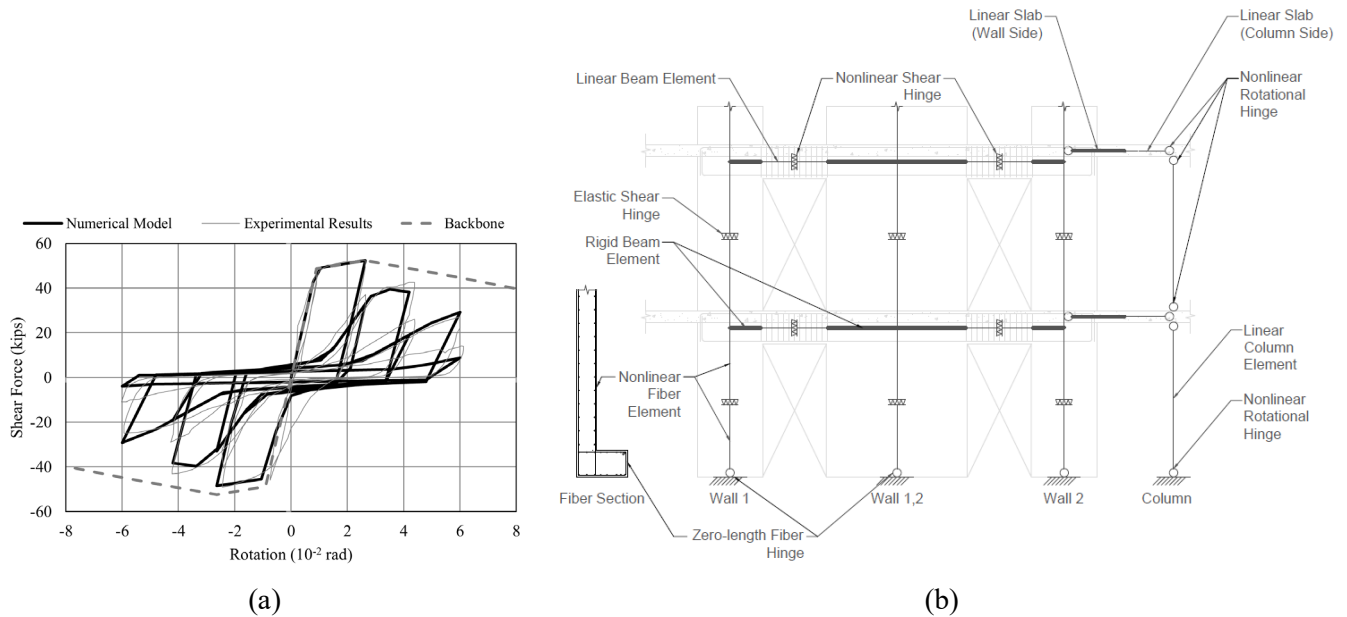


Fig. 2 - a) Nonlinear shear hinge model for the header beams, and b) typical storey of the OpenSees model

### 3. Ground Motion Suites

#### 3.1 Methodology

The methodology from Fairhurst et al. [17] was adopted in order to match a mean target spectrum and target lognormal standard deviation. Since 2-component motions were required for the subsequent 3D NDA, the method was modified to work on the geomean of the motions, rather than individual components. A basic summary of the methodology is:

- 1) Seed records with appropriate metadata (site class, distance, magnitude) are selected and scaled to the target mean spectrum.
- 2) A period-dependent factor function:  $FF(T)$ , between the spectrum:  $SA_{target}(T)$ , and seed geomean spectra:  $SA_{geo}(T)$ , is computed:

$$FF(T) = SA_{target}(T)/SA_{geo}(T) \quad (1)$$

Note:  $SA_{geo}(T)$  refers to the geometric mean of the suite of geomean spectra.

- 3) A variable target spectrum (VTS) [18]:  $VTS_i(T)$ , is computed for each record,  $i$ , by multiplying the seed record's geomean spectrum:  $SA_i(T)$ , by the factor function at each period:

$$VTS_i(T) = FF(T) \cdot SA_i(T) \quad (2)$$



- 4) Each  $VTS_i(T)$  is modified by a single linear function in log-space to adjust the standard deviation of the suite at each period,  $T$ , while leaving the mean unchanged:

$$\ln(VTS^*_i(T)) = \ln(VTS_i(T)) \cdot \sigma_{\text{target}}(T)/\sigma_{VTS}(T) - \mu_{VTS}(T) \cdot \sigma_{\text{target}}(T)/\sigma_{VTS}(T) + \ln(SA_{\text{target}}(T)) \quad (3)$$

where  $VTS^*_i(T)$  is the modified VTS for record;  $\sigma_{\text{target}}(T)$  is a target lognormal standard deviation,  $\sigma_{VTS}(T)$  is the lognormal standard deviation of the suite of  $VTS_i(T)$  before modification, and  $\mu_{VTS}(T)$  is the lognormal mean of the suite of VTS before modification.

- 5) Finally, each seed record is spectrally matched to its target  $VTS^*_i(T)$ . This was done using existing spectral matching techniques implemented in RSPMatch v05 [19]. The resulting suite of matched records will match both the target mean spectrum and target lognormal standard deviation.

The advantages of this method are twofold:

- 1) When limited records are available (i.e. large magnitude subduction records), seed records with imperfect spectra can be selected, as the method will adjust the suite to match the target.
- 2) Spectral variation is controlled by setting a target lognormal standard deviation. This makes the comparison of results derived for different suites comparable.

For this study, the target spectrum was taken as the 2020 Vancouver, Site Class C ( $V_{s30} = 450$  m/s), uniform hazard spectrum (UHS); the target lognormal standard deviation was taken from the suite of crustal ground motion models (GMMs) adopted to produce the UHS [20].

### 3.2 Crustal Suite

NEHRP Site Class C records were selected from the PEER NGA-West2 database [21]. Magnitude 5.5-7.5 events recorded at 0-80 km were selected based on disaggregation results at 1.1 s. The selected 15 crustal records are listed in Table 1.

Table 1 - Seed Record Summary

Crustal				Interface			
Earthquake	Mag	Year	Station	Earthquake	Mag	Year	Station
Chi-Chi	6.2	1999	CHY029	Maule	8.8	2010	LaFlorida
Chi-Chi	6.2	1999	TCU	Maule	8.8	2010	Penalolen
Northridge	6.69	1994	5108	Maule	8.8	2010	Matanzas
Coalinga	6.36	1983	COW	Maule	8.8	2010	Hualane
Loma Prieta	6.93	1989	HSP	Maule	8.8	2010	SJCH
Tabas	7.35	1978	TAB	Tohoku	9.1	2011	CHB013
Chi-Chi	6.2	1999	TCU070	Tohoku	9.1	2011	AOM021
Tabas	7.35	1978	DAY	Tohoku	9.1	2011	YMT002
Cape Mendoza	7.01	1992	FOR	Tohoku	9.1	2011	AKT018
Chi-Chi	6.2	1999	CHY034	Tohoku	9.1	2011	MYG005
Northridge	6.69	1994	FAI	Tohoku	9.1	2011	AKT006
Mammoth	5.91	1988	CVK	Hokkaido	8.3	2003	HKD129
Landers	7.28	1992	LCN	Hokkaido	8.3	2003	HKD039
Landers	7.28	1992	NPS	Hokkaido	8.3	2003	HKD105
Duzce	7.14	1999	BOL	Michoacán	8.1	1985	AZIH



The geomean of the seed records was matched to the target UHS and lognormal standard deviation using the previously described methodology from 0.1 – 3.5 s. The resulting seed and matched suite spectra are illustrated in Figure 3.

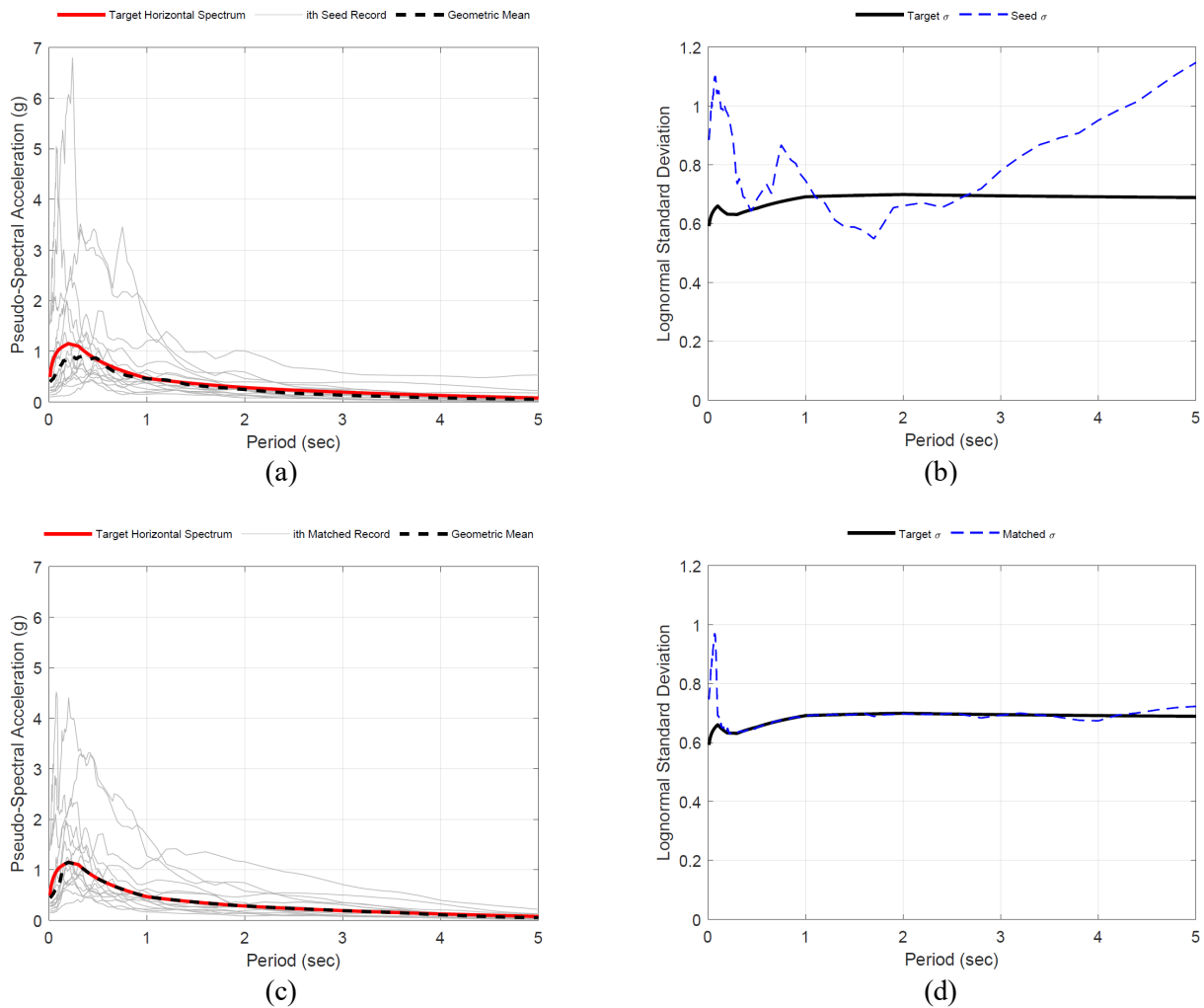


Fig. 3 – Crustal suite matching summary: a) seed suite geomean spectra; b) seed suite geomean lognormal standard deviation; c) matched suite geomean spectrum; and d) matched suite geomean lognormal standard deviation.

### 3.3 Subduction Interface Suite

The S<sup>2</sup>GM database [22], supplemented with additional subduction records from the K-Net Japanese record database [23], was used as a record source for the subduction interface records. Site Class C records at distances of 30-150 km from magnitude 8+ events were considered for the subduction interface suite development.

The same period range as used for the crustal suite (0.1 – 3.5 s) was used for spectral matching the seed records to their target. The resulting subduction suite spectra are illustrated in Figure 4. The seed records are listed in the second column of Table 1.

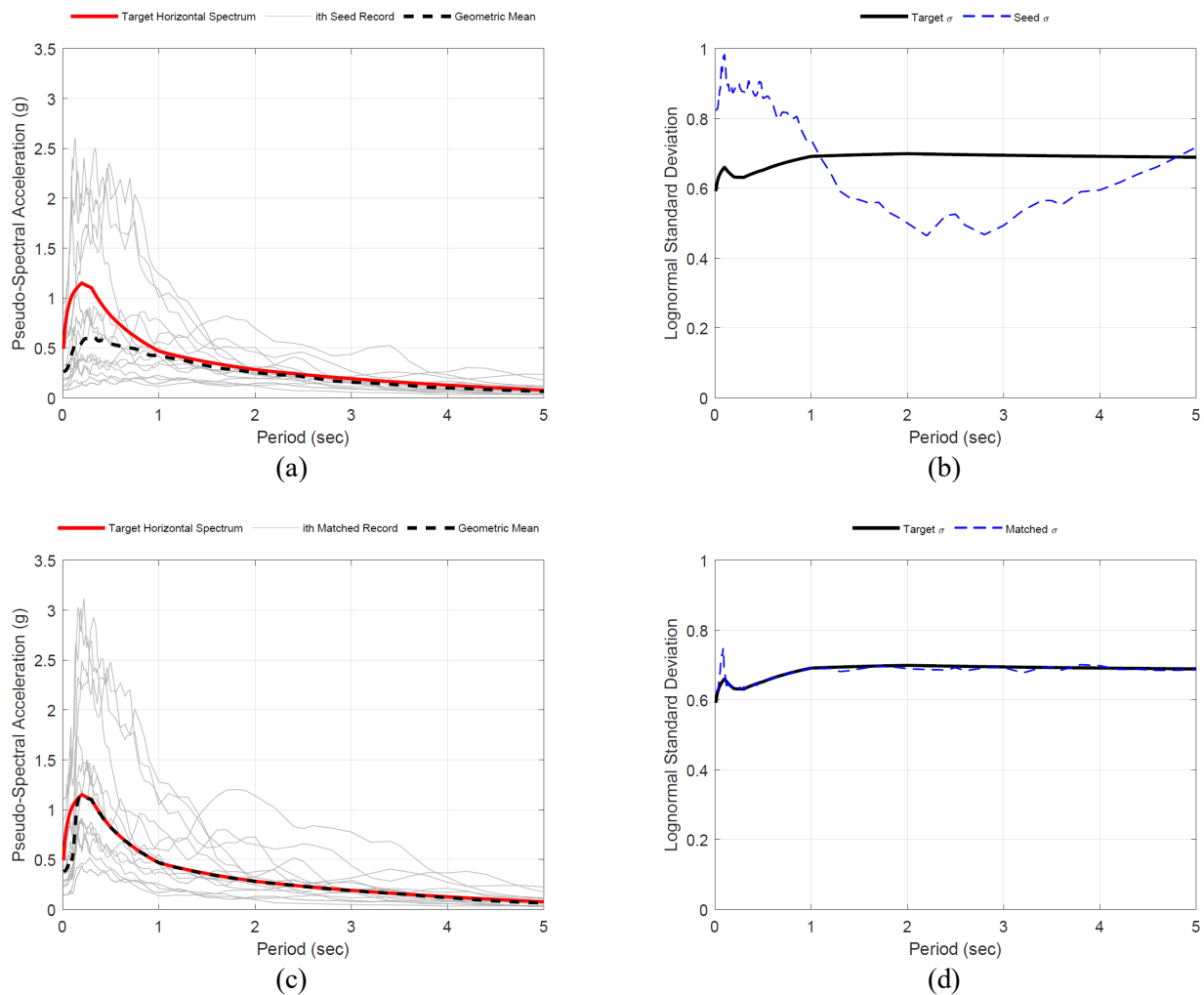


Fig. 3 – Subduction interface suite matching summary: a) seed suite geometric mean spectra; b) seed suite geometric mean lognormal standard deviation; c) matched suite geometric mean spectrum; and d) matched suite geometric mean lognormal standard deviation.

#### 4. Analysis Results

NDA was performed using both suites of matched motions. Figures 4 and 5 present the individual motion interstory drifts and the mean from each suite in the coupled and non-coupled directions, respectively. The NBCC uses interstory drifts as a surrogate for structural damage and limits regular buildings to a mean maximum interstory drift of 2.5% of the story height when using a suite of records to conduct time history analysis. For the collapse prevention evaluation used in performance-based design, the Los Angeles Tall Building Structural Design Council (LATBSDC) limits mean and maximum interstory drifts to 3.0% and 4.5%, respectively [9]. As seen in Figures 4 and 5, neither suite produces mean drifts that surpass these limits. From Figure 5, it can be seen that one subduction ground motion produces excessive drifts (collapse) in the non-coupled direction; other than this motion, the rest are all below the 4.5% limit.

Figure 6 plots the maximum header rotation at each story from each suite. For reference, the maximum allowable mean rotation for these headers, following ASCE 41-13, would be 0.03 radians. This limit is not exceeded by the mean of either suite.



The drift and header rotation demand from the subduction suite are slightly higher than the crustal records; however, are low in both cases. This is because the overall damage is quite low at this level of shaking. At these lower levels of damage, the amount of degradation in the walls and header beams is low, which will largely nullify the effect of the ground motion duration.

Finally, in Figure 7, total story shear forces are plotted from each suite (sum of shear in each wall). These results are similar in both suites since these forces are governed by the strengths of the walls. The individual shear forces in each wall are well below the wall shear capacities.

## 5. Conclusions

In this study, two suites of ground motions were developed for the 2020 2%/50-year hazard for Vancouver, BC: a long duration subduction suite and a short duration crustal suite. The mean and variation of the record suites were both matched to a target UHS and associated lognormal standard deviation to ensure a valid comparison solely of duration. The suites were used to run NDA on a 3D degrading model of an existing RC concrete shearwall building. The model was able to capture both nonlinear second order effects and all major modes of degradation for this structural system (concrete spalling, cracking and crushing; steel fatigue, buckling, slip, and rupture; and header beam cyclic and in-cycle degradation).

Both suites provide results that meet code (NBCC and LATBSDC17) limits; however, the long duration subduction motions were more demanding on average. This means that the code provisions used to design the archetype building were conservative enough to produce a safe design, even when subjected to the subduction motion suite. However, further analyses, including nonlinear incremental dynamic analysis (NIDA), should also be conducted to truly assess the collapse risk for this type of structure (i.e. FEMA P695 [24]).

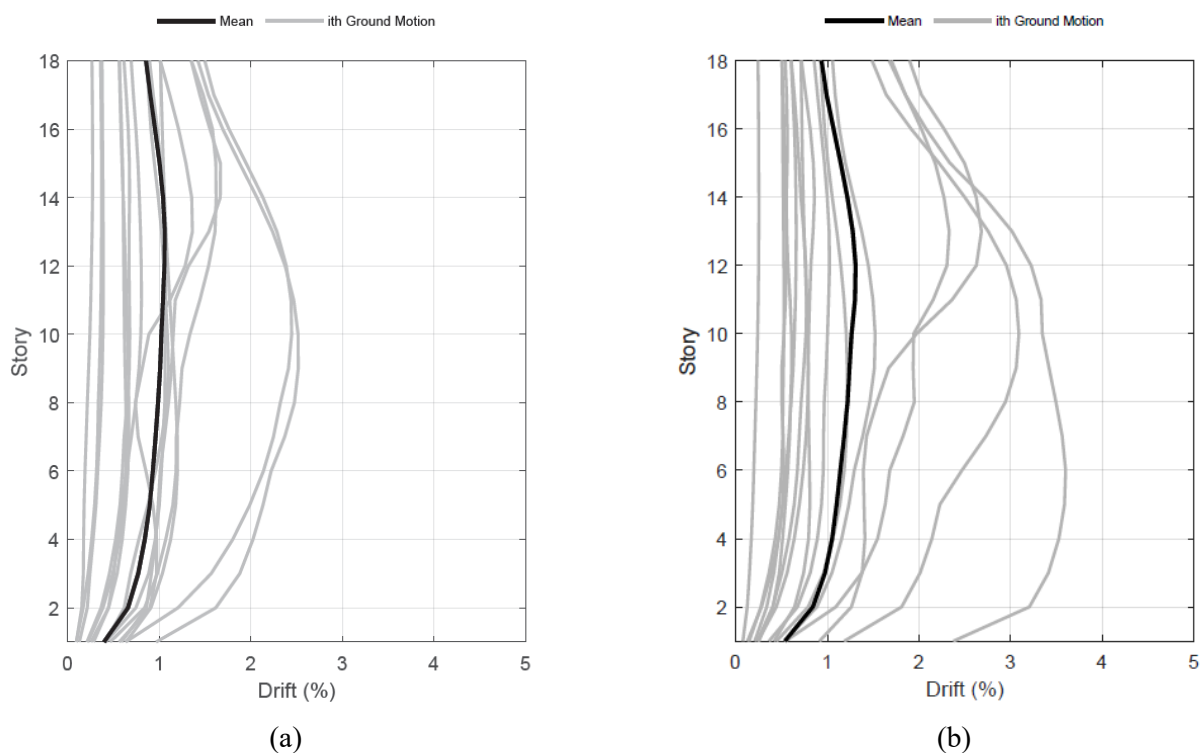


Fig. 4 – Interstory drifts in the coupled direction for a) the crustal suite; and, b) the subduction interface suite

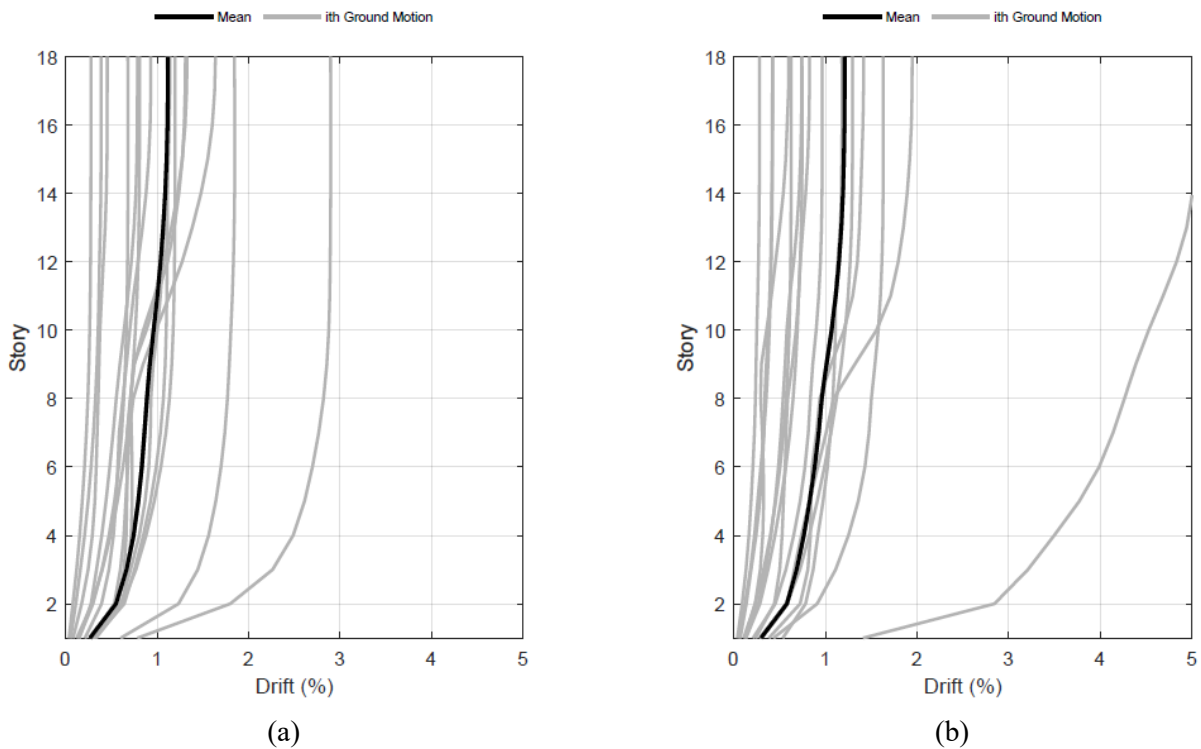


Fig. 5 – Interstory drifts in the non-coupled direction for a) the crustal suite; and, b) the subduction interface suite

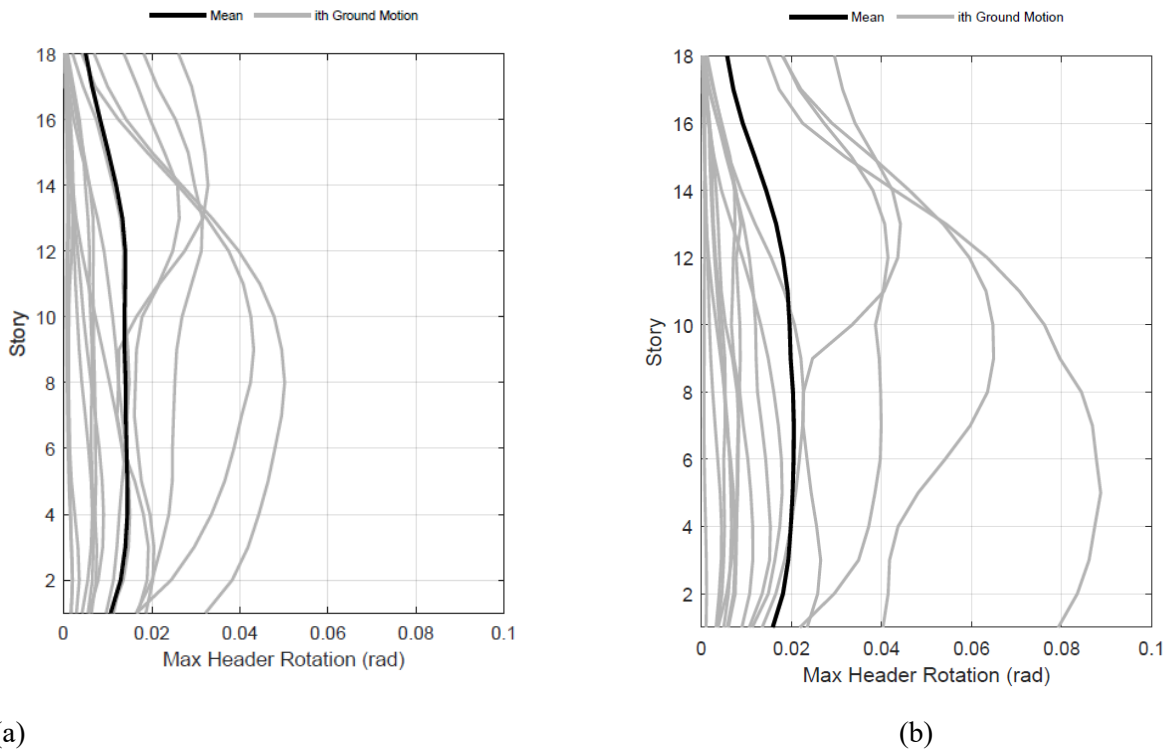


Fig. 6 – Maximum header rotations for a) the crustal suite; and, b) the subduction interface suite

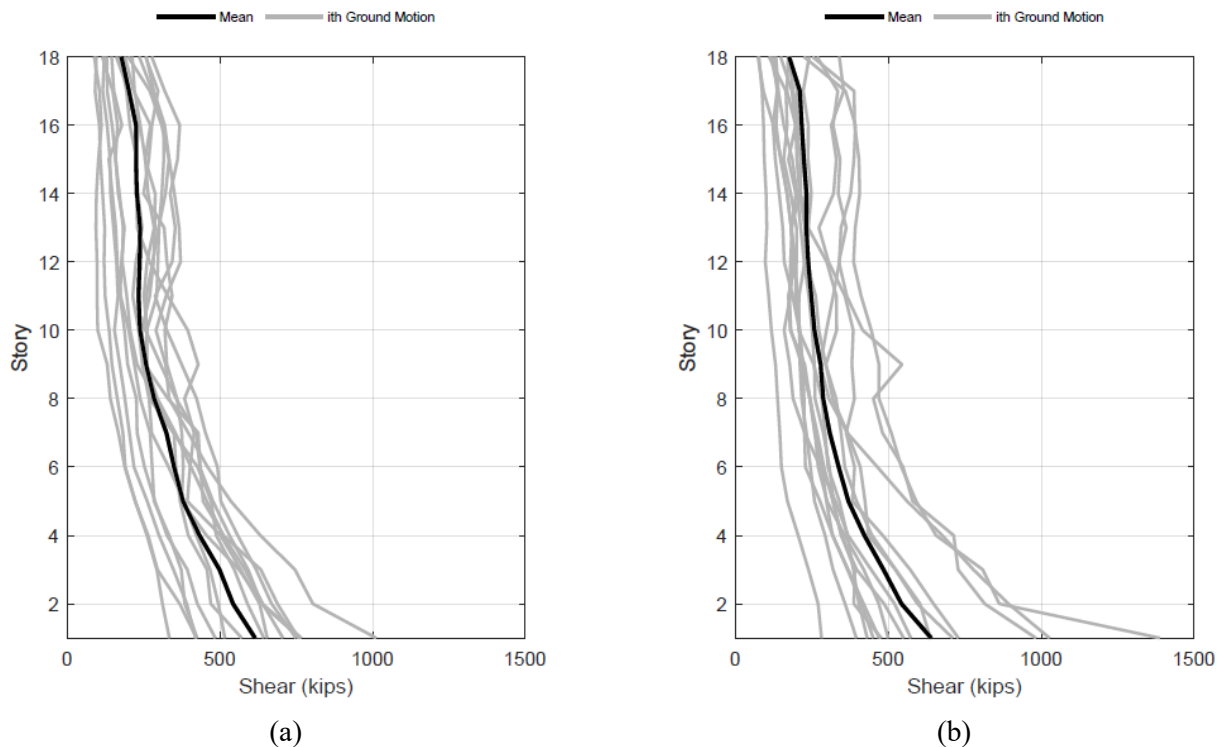


Fig. 7 – Maximum story shear forces for a) the crustal suite; and, b) the subduction interface suite

## 6. Acknowledgements

The study in this paper is part of the PhD dissertation of the first author which was funded by the Natural Sciences and Engineering Research Council of Canada (NSERC).

## 7. References

- [1] Goldfinger C, Nelson CH, Morey AE, Johnson JE, Patton JR, Karabanov E, Gutierrez-Pastor J, Eriksson AT, Gracia E, Dunhill G, Enkin RJ (2012): *Turbidite event history: Methods and implications for Holocene paleoseismicity of the Cascadia subduction zone*. US Geological Survey Professional Paper, 1661.
- [2] Chandramohan R, Baker JW, Deierlein GG (2016): Impact of hazard-consistent ground motion duration in structural collapse risk assessment". *Earthquake Engineering and Structural Dynamics*, **45** (8), 1357-1379.
- [3] Chandramohan R, Baker JW, Deierlein GG (2016): Quantifying the influence of ground motion duration on structural collapse capacity using spectrally equivalent records. *Earthquake Spectra*, **32** (2), 927-950.
- [4] Fairhurst M, Bebmazadeh A, Ventura CE (2019): Effect of ground motion duration on reinforced concrete buildings. *Earthquake Spectra*, **35** (1), 311-331.
- [5] Raghunandan M, Liel AB (2013): Effect of ground motion duration on earthquake-induced structural collapse. *Structural Safety*, **41**, 119-133.
- [6] NRCC (2010): *National Buildings Code of Canada*. National Research Council of Canada, Ottawa, Ont., Canada.
- [7] McKenna F, Fenves GL, Scott MH, Jeremic B (2000): *Open System for Earthquake Engineering (OpenSees)*, Pacific Earthquake Engineering Research Center, Berkeley, Ca.
- [8] Pugh J (2012): *Numerical Simulation of Walls and Seismic Design Recommendations for Walled Buildings*. Doctoral Dissertation, University of Washington, Seattle, Wa.



- [9] LATBSDC (2017): *An Alternative Procedure for Seismic Analysis and Design of Tall Buildings Located in the Los Angeles Region*. Los Angeles Tall Building Structural Design Council, Los Angeles, Ca.
- [10] Galano L, Vignoli A (2000): Seismic behavior of short coupling beams with different reinforcement layouts. *ACI Structural Journal* **97** (6), 876-885.
- [11] Lowes LN, Mitra N, Altoontash A (2004): *A Beam-column Joint Model for Simulating the Earthquake Response of Reinforced Concrete Frames*, PEER Report 2003/10. Pacific Earthquake Engineering Center (PEER), University of California, Berkeley, Ca.
- [12] Yassin MHM (1994): *Nonlinear Analysis of Prestressed Concrete Structures under Monotonic and Cyclic Loads*, Doctoral Dissertation, University of California, Berkeley, Ca.
- [13] Mander JB, Priestley MJ, Park R (1988): Theoretical stress-strain model for confined concrete. *Journal of Structural Engineering*, **114** (8), 1804-1826.
- [14] Brown J, Kunnath SK (2000): *Low Cycle Fatigue Behavior of Longitudinal Reinforcement in Reinforced Concrete Bridge Columns*, NCEER Technical Report 00-0007. National Center for Earthquake Engineering Research, State University of New York at Buffalo, Buffalo, NY.
- [15] Zhao J, Sritharan S (2007): Modeling of strain penetration effects in fiber-based analysis of reinforced concrete structures. *ACI Structural Journal*, **104** (2), 133-141.
- [16] ASCE/SEI (2013). *Seismic Evaluation and Retrofit of Existing Buildings*. American Society of Civil Engineering/Structural Engineering Institute, ASCE 41-13, Reston, Va.
- [17] Fairhurst M, Bebmazadeh A, Ventura CE (2019): An algorithm for the development of hazard consistent record suites: example for subduction megathrust records. *In press*.
- [18] Seifried AE (2013): *Response compatibilization and impact on structural response assessment*. Doctoral dissertation, Stanford University, Ca.
- [19] Hancock J, Watson-Lamprey J, Abrahamson NA, Bommer JJ, Markatis A, McCoy E, Mendis R (2006): An improved method of matching response spectra of recorded earthquake ground motion using wavelets. *Journal of Earthquake Engineering*, **10** (1), 67-89.
- [20] Adams J, Allen TI, Halchuk S, Kolaj M (2019): Canada's 6th generation seismic hazard model, as prepared for the 2020 National Building Code of Canada. *12th Canadian Conference on Earthquake Engineering CCEE12*, Quebec City, Qc., Canada.
- [21] Ancheta TD, Darragh RB, Stewart JP, Seyhan E, Silva WJ, Chiou BS, ... Kishida T (2013): *Peer NGA-West2 database*. Pacific Earthquake Engineering Research Center (PEER), Berkeley, Ca.
- [22] Bebamzadeh A, Ventura CE, Fairhurst M (2015): S<sup>2</sup>GM: A tool for ground motion selection and scaling ground motion records. *2015 Los Angeles Tall Building Structural Design Council Annual Meeting*, Los Angeles, Ca.
- [23] Kinoshita S (1998): Kyoshin Net (K-net). *Seismological Research Letters*, **69** (4), 309-332.
- [24] FEMA (2009): *Quantification of Building Seismic Performance Factors*, Federal Emergency Management Agency, Washington, DC.